Inhibition of lysophosphatidic acid acyltransferase β disrupts proliferative and survival signals in normal cells and induces apoptosis of tumor cells

Michael Coon,[1] Alexey Ball,[1] Jeannine Pound,[1] Sophe Ap,[1] David Hollenback,[1] Thayer White,[1] John Tulinsky,[1] Lynn Bonham,[1] Deborah K. Morrison,[2] Robert Finney,[3] and Jack W. Singer[1]

[1] Cell Therapeutics, Seattle, WA; [2] Regulation of Cell Growth Laboratory, NCI-Frederick, MD; and [3] PanGenex, Seattle, WA

Abstract

Lysophosphatidic acid acyltransferase β (LPAAT-β) is an intrinsic membrane protein that catalyzes the synthesis of phosphatidic acid (PA) from lysoPA. Given that PA is a cofactor in a number of signaling cascades that are constitutively active in tumors, we evaluated the role of PA produced by LPAAT-β in *Xenopus* oocyte meiotic maturation assays and an isoform-specific inhibitor of LPAAT-β in mammalian cell assays. We found that ectopic overexpression of LPAAT-β cooperates in activation of the Ras/Raf/Erk pathway in *Xenopus* oocytes and that inhibition of LPAAT-β inhibits signaling in both the Ras/Raf/Erk and PI3K/Akt pathways. When LPAAT-β activity is suppressed by CT32228 (*N*-(4-bromo-phenyl)-6-(5-chloro-2-methyl-phenyl)-[1,3,5]triazine-2,4-diamine), an isoform-specific noncompetitive inhibitor, tumor cells undergo mitotic catastrophe while most normal cells simply arrest or become quiescent. The data presented here suggest that PA produced by LPAAT-β plays an important role in signaling pathways critical to tumor cell survival. (Mol Cancer Ther. 2003;2:1067–1078)

Introduction

Lysophosphatidic acid (LPA) is converted to phosphatidic acid (PA) by acylation of the *sn*-2 position by LPA acyltransferase (LPAAT) activity. Several enzymes with LPAAT activity have been described including LPAAT-α (1), LPAAT-β (1), Endophilin (2), and CtBP/BARS (3). The PA produced by LPAAT activity can become a substrate for lipid phosphate phosphohydrolase in the production of diacylglycerol (DAG) or as a substrate of CDP-DAG synthase and thus to other phospholipid synthetic pathways. PA is also produced by the activity of phospholipase D1 and D2 (PLD) and DAG kinase (DAGK) (4). In addition to its role in lipid biosynthesis, PA has been implicated in a number of signaling pathways, including Raf translocation to membranes (5), mTOR activation (6), epidermal growth factor receptor (EGFR) internalization (7), vesicle formation (8), regulation of the non-receptor tyrosine kinase Fgr (9), activation of PKCζ (10), and the association of phospholipase C (PLC) with membranes (11). However, specific approaches to define of the origin of signaling-associated PA have been lacking.

PA produced by the activity of PLD1 or PLD2 or both is thought to affect numerous cellular pathways including organization of the cytoskeleton, respiratory bursts, proliferation, and release of cytokines and other extracellular modulators. PLD activity has been shown to be important in several signaling pathways including p38 mitogen-activated protein kinase (MAPK) activity in activated promyeloblasts (12), hydrogen peroxide-induced apoptosis in rat pheochromocytoma cells (13), and sphingosine-1-phosphate-mediated activation of the EDG3 receptor (14), all suggesting that PLD-derived PA plays distinct roles in some signaling pathways. Although DAGK phosphorylates DAG to produce PA, the principle function of DAGK in signaling pathways appears to be attenuating signals propagated by the secondary messenger DAG rather than augmenting the effects of PA (15–18). Endophilin, a dynamin-binding protein shown to play an important role in endocytosis and recycling of synaptic vesicles, has LPAAT activity (2, 19). CtBP/BARS is reported to have LPAAT activity that is important for fission of Golgi membranes (3).

LPAAT-α is ubiquitous and expressed uniformly in all tissues tested, while LPAAT-β has a more distinct and differential tissue distribution, principally in the liver and heart and to a lesser extent in hormone responsive tissues such as the prostate, ovaries, and testis (20–22). LPAAT-β is expressed at high levels in a wide variety of tumor cells and their surrounding stroma but has restricted expression in normal cells; it is found at relatively high levels in endothelial cells, vascular smooth muscle cells, and stromal cells derived from hormone responsive tissue (23). LPAAT-α is thought to be located primarily in the endoplasmic reticulum (ER) (24) although its activity has been observed in mitochondria (25). The precise intracellular localization of LPAAT-β is unclear but our observations show that it is located primarily in the ER. The tissue distribution and differential levels of expression of LPAAT-β compared to LPAAT-α suggest that LPAAT-β may play specialized roles distinct from LPAAT-α.

We investigated whether PA generated from LPAAT-β contributes to signaling pathways. We show here that LPAAT-β, but not LPAAT-α or PLD, cooperated with Raf and Ras in the induction of germinal vesicle breakdown (GVBD) in *Xenopus* oocytes, which resulted in enhanced

Received 3/12/03; revised 5/19/03; accepted 6/20/03.

The costs of publication of this article were defrayed in part by the payment of page charges. This article must therefore be hereby marked advertisement in accordance with 18 U.S.C. Section 1734 solely to indicate this fact.

Requests for Reprints: Michael Coon, Cell Therapeutics, Seattle, WA 98117. E-mail: mcoon@ctiseattle.com

Erk activation. To investigate how inhibition of LPAAT-β may perturb signaling pathways in mammalian cells, we developed isoform-specific low nanomolar inhibitors of LPAAT-β. Treatment with one such compound, CT32228 (*N*-(4-bromo-phenyl)-6-(5-chloro-2-methyl-phenyl)-[1,3,5]triazine-2,4-diamine), resulted in inhibition of signaling pathways in relevant primary cell models of growth factor and cytokine-induced response. The results show that in these normal cells, inhibition of LPAAT-β attenuates both Ras/Raf/Erk and PI3K/Akt signal transduction pathways. In tumor cells, treatment with CT32228 results in accumulation of cells in G_2-M followed by mitotic catastrophe and apoptosis. Our results suggest that PA derived from LPAAT-β activity is an important cofactor in a number of signaling pathways and that tumor cells are more sensitive to the loss of this source of PA than are some normal cells.

Materials and Methods

Reagents

Angiotensin II (Ang II), vascular edothelial growth factor (VEGF) receptor tyrosine kinase inhibitor, AT_1R antagonist, and VEGF were obtained from Calbiochem, La Jolla, CA. Antibodies to Erk2, Raf-1 mTOR(FRAP), and Akt were obtained from Santa Cruz Biotechnology, Santa Cruz, CA. Antibodies to Cdc2, Wee1, and DR4/TRAILR-1 were obtained from Upstate Biotechnology, Waltham, MA. Antibodies to DR5/TRAILR-2 were obtained from Cayman Chemical, Ann Arbor, MI. Antibodies to phosphorylated Erk1/2(Y^{204}/T^{202}), $p70^{S6K}$(T^{421}/S^{424}), $p70^{S6K}$(S^{65}), Cdc2(Y^{15}), Cdc2(T^{161}), mTOR(S^{2448}), Akt(S^{473}), $p90^{RSK}$(T^{359}/S^{363}), pro-Caspase 3, Caspase 8, Caspase 9, pro-Caspase 10, BAX, and the PI3K inhibitor LY294002 were obtained from Cell Signalling Technologies, Beverly, MA. Monoclonal antibodies LPAAT-β (4B12) and rabbit polyclonal antisera were made for Cell Therapeutics by Covance Research Products, Denver, PA.

Oocyte Injection and Analysis

Oocytes were isolated and defolliculated as previously described (26). Within 18 h of isolation, 30 ng of *in vitro* transcribed RNA encoding the various LPAAT proteins were injected into oocytes. Eight to 12 h later, 30 ng of either $Raf1^{Y340D}$ or $Ha\text{-}Ras^{V12}$ RNA were then injected into the oocytes. Oocytes were scored for GVBD, as evidenced by the appearance of a white spot at the animal pole. This observation was verified by manual dissection of oocytes after fixation in 8% trichloroacetic acid. For biochemical analysis, oocytes were lysed (10 μl per oocyte) by trituration with a pipette tip in either NP40 buffer [20 mM Tris (pH 8.0), 137 mM NaCl, 10% v/v glycerol, 1% v/v NP40, 2 mM EDTA, aprotinin (0.15 units/ml), 1 mM phenylmethylsulfonyl fluoride (PMSF), 20 μM leupeptin, 5 mM sodium vanadate] or RIPA buffer [20 mM Tris (pH 8.0), 137 mM NaCl, 10% v/v glycerol, 1% v/v NP40, 0.5% sodium deoxycholate, 0.1% w/v SDS, 2 mM EDTA, aprotinin (0.15 units/ml), 1 mM PMSF, 20 μM leupeptin, 5 mM sodium vanadate]. Lysates were cleared by centrifugation at 14,000 × *g* for 5 min at 4°C.

LPAAT Enzymatic Activity

For measurement of LPAAT activity in frog oocytes, 11 oocytes were homogenized in 200 μl of ice-cold homogenization buffer [20 mM HEPES (pH 7.5), 1 mM EDTA, 1 mM benzamidine, and 1 μg/ml each soy bean trypsin inhibitor, Pepstatin A, and leupeptin] with 6 strokes of a Duall homogenizer. The samples were centrifuged at 1500 × *g* for 2 min at 4°C and the supernatant was saved for protein quantification with the bicinchoninic acid (BCA) assay (Pierce, Rockford, IL) and for the LPAAT assay. LPAAT activity was measured by formation of PA during a 7-min incubation period at 37°C in 12 × 75 mm borosilicate test tubes containing 50 μl of 50 mM HEPES (pH 7.5), 100 mM NaCl, 1 mM EDTA, 1 mg/ml fatty acid-free BSA, 0.25 mM ^{14}C-labeled 18:1-CoA (about 40,000 cpm/assay), 0.25 mM *sn*-1-18:1 lysoPA, and 0.001–0.05 mg/ml of oocyte homogenate. Assays were quenched by the addition of 1.3 ml of chloroform/methanol/HCl = 48/51/0.7. Carrier lipids (10 μg) were added and the phases were separated with the addition of 0.35 ml water. The upper phase was discarded and the lower phase was dried under nitrogen. ^{14}C-labeled PA was separated from ^{14}C-labeled 18:1-CoA by TLC on Analtech silica gel 60 HP-TLC plates in chloroform/methanol/acetic acid/water = 85/12.5/12.5/3 essentially as described (27) and was quantitated by exposing the TLC plates to a phosphor screen (Molecular Dynamics, Piscataway, NJ). LPAAT activity was linear with time and protein.

A second LPAAT assay was performed to screen for LPAAT-β inhibitors and subsequently determine IC_{50} values. These assays were performed at room temperature in flat-bottom, MicroWell 96-well polystyrene plates (Nunc, Rochester, NY). Activities were determined using separate SF9 membrane preparations containing overexpressed human LPAAT-α or human LPAAT-β isozymes (0.015 mg/ml protein), 200 μM of 18:1-CoA, 200 μM *sn*-1-18:1 lysoPA, 500 μM DTNB, 25 mM HEPES, pH 7.5, 1 mM EDTA, 1 mg/ml BSA, 100 mM NaCl, and various concentrations of CT32228. The compound was added in 8 μl of DMSO, and the total reaction volume was 100 μl. Product formation was monitored by the change in absorbance at 405 nm over 3 min on a Bio-Tek EL_x808 Microplate Reader and was linear with time and protein concentration. The computer program Prism (GraphPad Software Incorporated, San Diego, CA) used nonlinear regression to calculate the IC_{50} values.

Cell Culture

Human microvascular endothelial cells (HMVEC) were obtained from Clonetics/BioWhittaker, East Ruthersford, NJ, and cultured in EBM-2, supplemented with 0.001 mg/ml hydrocortisone, 0.05 mg/ml gentamicin, 0.05 μg/ml amphotericin-B, constituents of EGM-2MV (Cambrex, East Rutherford, NJ) endothelial cell supplement kit (hEGF, hFGF-B, VEGF, ascorbic acid, long R^3-Igf-1, heparin), and 5% fetal bovine serum (FBS). Baboon aortic vascular smooth muscle cells (PAVSMC) were prepared from *Papio cynocephalus* aortae by explant (kindly provided by G. Daum, University of Washington, Seattle,

WA) and cultured in DMEM supplemented with 10% FBS. Human aortic vascular smooth muscle cells (HAVSMC) were obtained from Clonetics/BioWhittaker and maintained in SmGM-3 media (Cambrex) plus 10% FBS. Before stimulation with growth factors or cytokines, cells were serum starved (0.5% BSA) for 16–24 h. Cells stimulated with VEGF required co-incubation with 1 ng/ml heparin.

Cell Lysate Preparation and Membrane Fractionation

Cells were harvested and lysed in detergent-containing lysis buffer [20 mM Tris-HCl (pH 8.0), 10 mM EGTA, 2 mM EDTA, 2 mM DTT, 1% v/v NP40, 1× Phosphatase Inhibitor Cocktail II (Sigma, St. Louis, MO), 1× Protease Inhibitor Cocktail (Sigma)], then clarified at 14,000 × *g* for 30 min at 4°C for analysis of whole cell lysates. In some experiments, a portion of each sample was lysed in buffer without detergent by sonication and clarified at 4000 × *g* for 30 min at 4°C to remove nuclei. Supernatants from cells lysed without detergent were centrifuged at 100,000 × *g* for 1 h at 4°C to sediment membranes. Supernatants consisting of the cytosolic fractions were removed and the crude membrane pellets were washed twice with ice-cold lysis buffer without detergent. Membrane pellets were disrupted by sonication in lysis buffer with 1% v/v Triton X-100, and then centrifuged at 100,000 × *g* for 1 h at 4°C to sediment detergent insoluble membrane fractions. Supernatants were saved for membrane-associated protein analysis.

Immunoblotting

Samples were normalized for protein concentration as measured by the BCA assay (Pierce). Proteins were separated by SDS-PAGE gels and electroblotted to polyvinylidene difluoride (PVDF) membranes using standard techniques. Primary antibodies were detected with horseradish peroxidase-coupled secondary antibodies (Amersham Pharmacia Biotech, Piscataway, NJ). Immunoblotting used an ECL detection kit (Amersham Pharmacia Biotech).

Cytotoxicity and Proliferation Assays

Proliferation was measured at a 72-h end point and was determined using a fluorescence-based measure of DNA synthesis (CyQuant Cell Proliferation Kit, Molecular Probes, Eugene, OR). Cytotoxicity was determined by relative incorporation of the nucleic acid vital stain Sytox Green (Molecular Probes) into cells after 72 h.

Flow Cytometric Analysis of Apoptosis and Cell Cycle

Apoptosis was assessed by staining cells with Annexin V conjugated to FITC (BD Biosciences Clontech, Palo Alto, CA). As a control for necrosis, Annexin V-stained cells were counterstained with the vital dye, propidium iodide (Sigma). Genomic content of cells was assessed by propidium iodide staining of isolated nuclei. Briefly, cells were harvested, resuspended in 75% ethanol, and stored at −20°C until ready for analysis. Cells were then lysed in PI staining buffer [0.05 mg/ml propidium iodide, 7 units/ml RNase A, 0.001% v/v NP40, 10 mM NaCl, 5 mM Tris-HCl (pH 7.4)]. Relative fluorescence was measured on a Coulter Epics flow cytometer.

Mitotic Index and Caspase 3 ICC Staining

Cells were grown to ~70% confluence and then treated with either vehicle (DMSO) or CT32228 at a concentration equivalent to twice each cell type's IC_{50} for proliferation. Cells were collected at various times and imbedded in fibrinogen. Cells were then stained with H&E and the mitotic index was determined by counting the number of mitotic bodies visible in 10 representative high power fields (HPFs). Cells were also stained with anti-activated Caspase 3 antibody and detected with Vector Elite ABC Peroxidase kit (Vector Labs, Burlingame, CA).

Results

LPAAT-β Cooperates with Ras and Raf in the Induction of GVBD in *Xenopus* Oocytes

We first examined the role LPAAT-β plays in the Ras/Raf/Erk signaling pathway by using the *Xenopus* oocyte meiotic maturation assay. In this system, activation of the maturation promoting factor (MPF) is required for entry into the first meiotic phase and is dependent on Erk (28). Maturation of late prophase oocytes and entry into the first meiotic division was assessed by observations of GVBD. We microinjected *in vitro*-derived RNA transcripts from plasmid pSP64 Poly(A) vectors carrying LPAAT-β, LPAAT-α, or a catalytically inactive form of LPAAT-β (LPAAT-β^{R175A}) either alone or in combination with transcripts of constitutively active Raf (Raf1^{Y340D}). We found that LPAAT-β, but not LPAAT-α cooperated with constitutively active Raf in the induction of GVBD (Fig. 1A). Neither LPAAT isoform alone induced GVBD nor did the catalytically inactive form of LPAAT-β enhance Raf ^{Y340D}-induced GVBD. Importantly, injection of LPAAT-β transcripts significantly enhanced Raf1^{Y340D}-induced Erk phosphorylation while neither the catalytically inactive form of LPAAT-β nor LPAAT-α had any effect on Erk phosphorylation (Fig. 1A). LPAAT-β transcripts co-injected with oncogenic Ha-Ras^{V12} message also significantly enhanced GVBD while LPAAT-α had no effect (Fig. 1B). As with Raf1^{Y340D}-injected oocytes, co-injection of LPAAT-β with Ha-Ras^{V12} also resulted in increased MAPK activation. In this blot, Ha-Ras^{V12} appears as a doublet consisting of posttranslationally modified (upper) and unmodified (lower) bands. Microinjected transcripts are efficiently translated to comparable levels as judged by Western blots (Fig. 1C) and the LPAAT-injected oocytes had significant LPAAT activity (Fig. 1D). Due to the scale of the ordinate in Fig. 1D, the magnitude of LPAAT activity in some of the controls is unclear. Uninjected and Ha-Ras^{V12}-injected oocytes had LPAAT activities of 3.0 ± 2 and 2.4 ± 0.4 nmol min^{-1} mg^{-1}, respectively (Fig. 1D), comparable to some normal human cells (data not shown). Similar LPAAT activities were seen in the Raf1^{Y340D} experiments (data not shown). Microinjection of PLD transcripts had no effect on either Ha-Ras^{V12}- or Raf1^{Y340D}-induced GVBD (data not shown).

Treatment with CT32228 Is Cytotoxic and Antiproliferative to a Wide Variety of Tumor Cells

To further investigate whether LPAAT-β has a critical function related to tumor cell growth and/or viability, we

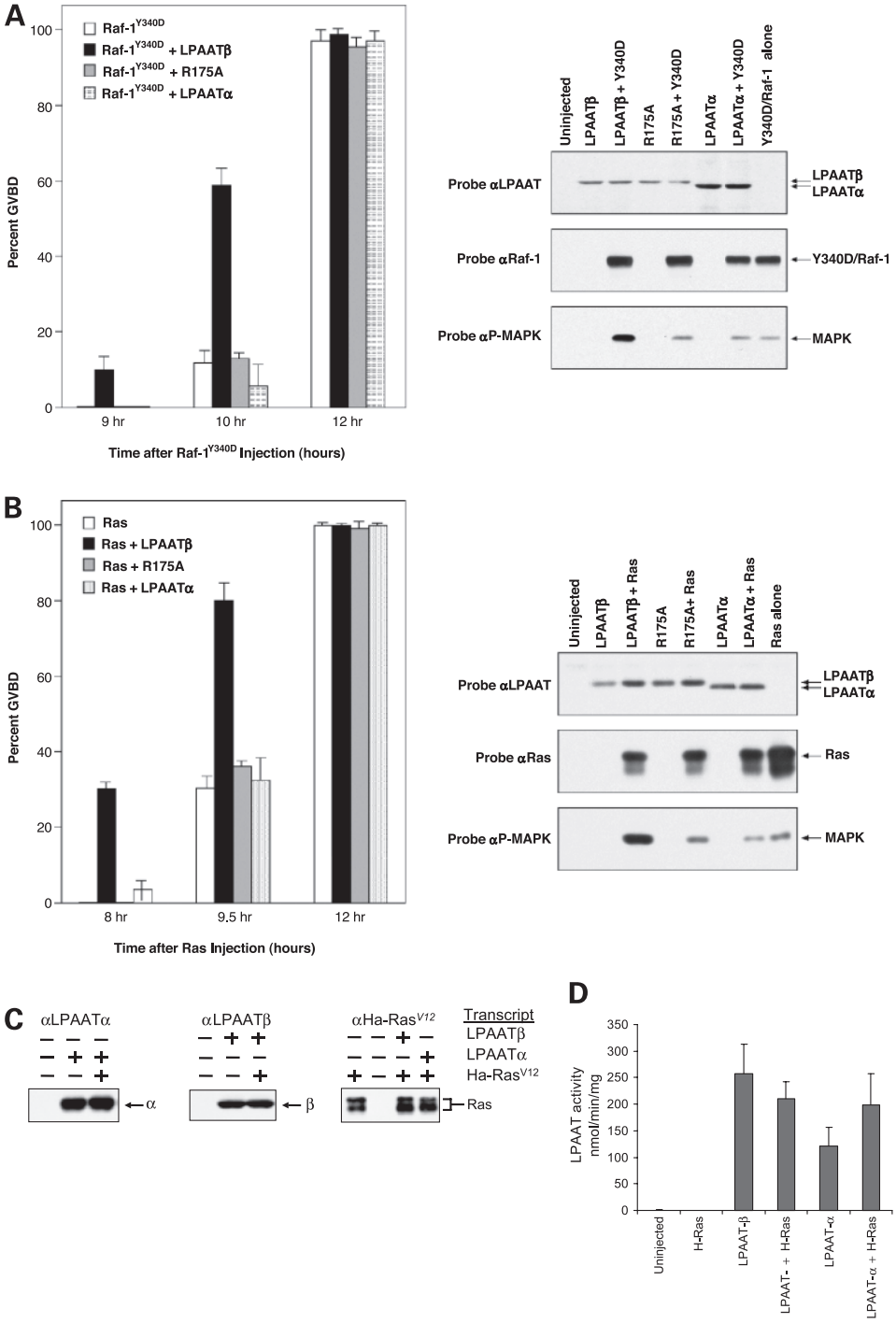

Figure 1. MAPK activation and germinal vesicle breakdown in *Xenopus* oocytes. *In vitro*-derived transcripts were injected into *Xenopus* oocytes and the number of oocytes undergoing GVBD at various times was scored. **A,** induction of GVBD with Raf transcripts. Transcripts of constitutively active Raf1^{Y340D}, LPAAT-α, or LPAAT-β alone were injected into oocytes, or Raf1^{Y340D} transcripts were co-injected with transcripts of LPAAT-α or LPAAT-β. Additionally, transcripts of catalytically inactive LPAAT-β^{R175A} were injected either alone or with Raf1^{Y340D} transcripts. Data are compiled from three separate experiments. Lysates from oocytes were prepared and subjected to Western analysis for MAPK activation. Samples are from transcript-injected oocytes as follows: *lane 1,* PBS control, *lane 2,* LPAAT-β; *lane 3,* LPAAT-β plus Raf1^{Y340D}; *lane 4,* LPAAT-β^{R175A}; *lane 5,* LPAAT-β^{R175A} plusRaf1^{Y340D}; *lane 6,* LPAAT-α; *lane 7,* LPAAT-α plus Raf1^{Y340D}; and *lane 8,* Raf1^{Y340D}. **B,** induction of GVBD with Ras transcripts. Transcripts of oncogenic Ha-Ras^{V12} either alone or with LPAAT-β or LPAAT-α transcripts were injected into oocytes. As controls, PBS vehicle control, LPAAT-β alone, or LPAAT-α alone were injected into oocytes. Data are compiled from three separate experiments. Lysates from oocytes were prepared and subjected to Western analysis for MAPK activation. Samples are from transcript-injected oocytes as follows: *lane 1,* PBS control; *lane 2,* LPAAT-β; *lane 3,* LPAAT-β plus Ha-Ras^{V12}; *lane 4,* LPAAT-β^{R175A}; *lane 5,* LPAAT-β^{R175A} plus Ha-Ras^{V12}; *lane 6,* LPAAT-α; *lane 7,* LPAAT-α plus Ha-Ras^{V12}; and *lane 8,* Ha-Ras^{V12}. **C,** Western analysis of transcript translation. Lysates from transcript-injected oocytes were probed with monoclonal antibodies to LPAAT-α (*left*), LPAAT-β (*middle*), or Ha-Ras^{V12} (*right*). **D,** LPAAT enzymatic activity. Injected oocytes were homogenized and tested for LPAAT enzymatic activity.

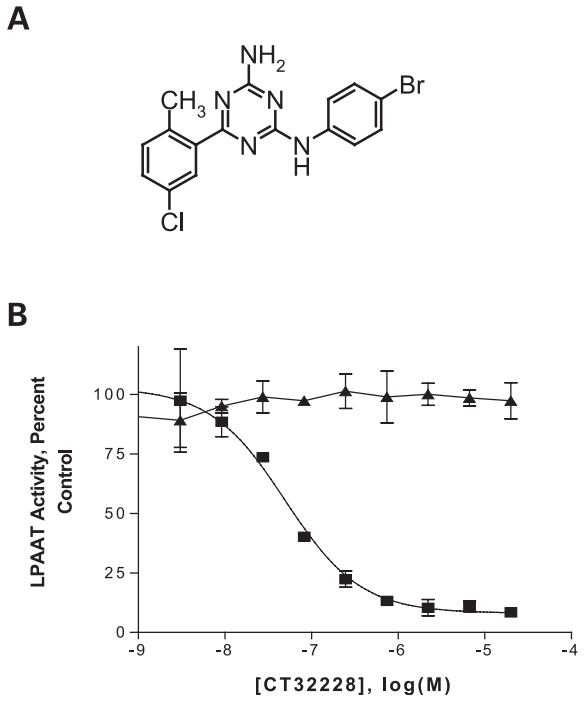

Figure 2. CT32228 specifically inhibits LPAAT-β. **A,** structure of CT32228. **B,** as part of a high-throughput screen, LPAAT activity was measured in SF9 insect membranes expressing human LPAAT-α (*filled triangles*) or LPAAT-β (*filled squares*) transgenes. The LPAAT-β specific IC_{50} for CT32228 in this experiment was approximately 50 nM. Typical control (wild type) SF9 membrane preps have an LPAAT activity of 2.9 ± 1.4 nmol min^{-1} mg^{-1}, while membranes from SF9 cells carrying LPAAT-α transgenes had activity of 1000 ± 140 nmol min^{-1} mg^{-1} and for those carrying LPAAT-β transgenes it was 1390 ± 200 nmol min^{-1} mg^{-1}.

treated a wide variety of normal and tumor cell lines with an LPAAT-β-specific mixed noncompetitive inhibitor, CT32228 (Fig. 2A). CT32228 is a member of a class of compounds that specifically inhibit LPAAT-β when compared to LPAAT-α in cell-free enzyme assays (Fig. 2B). CT32228 was derived by analogue synthesis following a high-throughput screen of an approximately 80,000 compound library. LPAAT-β is inhibited to comparable levels by CT32228 in intact cell assays (data not shown). CT32228 was potently antiproliferative and cytotoxic at nanomolar concentrations to almost all tumor cell lines tested (Table 1). CT32228 was antiproliferative to most normal cells but showed little to no cytotoxicity to several, most notably endothelial cells, VSMC, as well as immortalized rodent skeletal muscle cells (Table 2). Additionally, we found that normal human bone marrow progenitor cells are highly resistant to the antiproliferative effects of CT32228 (data not shown). Interestingly, CT32228 was cytotoxic to some primary and immortalized epithelial and fibroblast cell lines, suggesting that these cell types require LPAAT-β for survival.

Inhibition of LPAAT-β Activity Inhibits Raf Translocation

We examined the Ras/Raf/Erk pathway in mammalian cells to more clearly define LPAAT-β's function. Translocation of Raf from the cytosol to membranes is a necessary step before its activation and this translocation has been shown to be dependent on PA (29). Ang II, which exerts its effect in part through the Ras/Raf/Erk signaling pathway, is a pluripotent hormone with primary roles in angiogenic, contractile, and survival functions in HMVEC but is only weakly mitogenic. To determine if inhibition of LPAAT-β activity affects this signaling system, we fractionated lysates from Ang II-stimulated HMVEC that were either left untreated or pretreated for 45 min with 0.5 μM CT32228. We then assessed the degree of Raf translocation to the membrane-enriched fraction by Western blot analysis. Pretreatment with CT32228 significantly inhibited Raf translocation to membrane compartments (Fig. 3A). Erk phosphorylation in the same cells was significantly inhibited in a dose-dependent manner (Fig. 3B). Fluorescent microscopy experiments showed that CT32228 not only reduced the activation of Erk, but also resulted in significantly less accumulation of phosphorylated Erk in the nucleus (data not shown).

Erk1/2 Activation Is Inhibited by CT32228 in VEGF-Stimulated HMVEC

We also wanted to determine whether CT32228 could block additional signaling pathways in HMVEC such as that induced by VEGF. In VEGF-stimulated HMVEC, pretreatment with CT32228 inhibited Erk phosphorylation in a dose-dependent manner (Fig. 4A). Phosphorylation of $p90^{RSK}$ (T^{359}/S^{363}), a target of Erk, is also inhibited by CT32228 (Fig. 4B). Again, CT32228 was antiproliferative to HMVEC but was minimally cytotoxic to these cells (<5% at twice the IC_{50} at 72 h based on both Sytox assay and Caspase 3 IHC; data not shown).

The PI3K/Akt Survival Pathway Is Potently Inhibited in Ang II-Stimulated PAVSMC by CT32228

Ang II signals stimulate multiple signaling pathways in VSMC including Ras/Raf/Erk, PI3K/Akt, and Src family kinase-dependent pathways. AT_1 receptors (AT_1R) signal through a bifurcated pathway, one of which involves transactivation of the EGFR, thus activating the PI3K/Akt pathway (30). Because inhibition of LPAAT-β by CT32228 was cytotoxic to most tumor cell lines, but not to normal VSMC, we wanted to investigate effects on this survival pathway. As with HMVEC, CT32228 is potently antiproliferative to PAVSMC (IC_{50} = 125 nM) but is not cytotoxic even at concentrations greater than 1 μM (data not shown). We stimulated PAVSMC with Ang II either untreated or pretreated with CT32228. At 15 min post-stimulation with Ang II, Akt phosphorylation was profoundly inhibited by 500 nM CT32228 (Fig. 5A). This effect is seen as low as 125 nM CT32228 (data not shown). By 45 min, both Akt and Erk phosphorylation is diminished. As a positive control for PI3K inhibition in the assay, the PI3K-specific inhibitor LY490002 completely abolished Akt phosphorylation, while the AT_1R antagonist inhibited Akt phosphorylation to about the same level as CT32228. CT32228, however, does not inhibit Ang II transactivation of the EGFR (data not shown). Phosphorylation of downstream effectors of Akt, mTOR, $p70^{S6K}$, 4E-BP1, and GSK3β were inhibited by CT32228 and by LY490002 (Fig. 5B).

Table 1. Antiproliferative and cytotoxic effects of CT32228

Cell Line/Strain	Species, Tissue, Tumor/Normal	IC_{50} (nM)	LSCC (nM)
NMEC	human mammary, normal human mammary, immortal	100	<100
NMEC/E6E7	human mammary, immortal	100	<100
MCF-7	human mammary, tumor	100	100
PREC	human prostate, normal	25	25
NMEC/E6E7	human prostate, immortal	25	25
DU145	human pancreas, tumor	150	200
Panc-1	human pancreas, tumor	63	15
BxPC-3	human pancreas, tumor	125	125
CaOV-3	human ovary, tumor	200	100
CHO c-*sis*	hamster ovary, tumor	100	100
CHO cv-*sis*	hamster ovary, tumor	100	100
Colo201	human colon, tumor	100	ND
Lovo	human colon, tumor	50	250
LS174T	human colon, tumor	150	ND
HCT-116	human colon, tumor	63	125
NCI-H460	human lung, tumor	75	100
NCI-123	human lung, tumor	20	100
SVR	MS1 + Ha-*ras*, transformed	140	200
SVEC4-10	mouse microvessel, transformed	125	150
IP2E4	mouse microvessel, tumor	125	150
SK-MEL-2	human melanoma; N-*ras*, tumor	65	65
A2508	human melanoma; B-*raf*, tumor	50	50
SK-MEL-28	human melanoma; B-*raf*, tumor	150	ND
SK-MEL-31	human melanoma, tumor	500	ND
PrSC	human pros fb/stroma, normal	25	25
PrSC/E6E7	human pros fb/stroma, immortal	25	25
PC-12	rat adrenal gland, tumor	500	250
NIH/3T3	mouse embryo, immortal	150	150
NIH/3T3	mouse embryo, Ki-*ras* transformed	150	150
B1A	rat embryo, immortal	150	150
E12	rat embryo, H-*ras* immortal	150	150
ME-12	rat embryo, H-*ras* transformed	150	150

Note: The species, tissue, and whether the cell line has a tumor, normal or transformed phenotype are indicated. The IC_{50} for proliferation and the lowest significant cytotoxic concentration (LSCC) are indicated. IC_{50} is defined as the concentration at which proliferation is half-maximal to vehicle only controls. The LSCC is defined as that concentration which results in a significant increase in fluorescence compared to vehicle only-treated controls.

Table 2. Cell lines resistant to either or both the antiproliferative and cytotoxic effects of CT32228

Cell Line/Strain	Species, Tissue, Tumor/Normal	IC_{50} (nM)	LSCC (nM)
HAEC	human large vessel, normal	100	>500
HAEC/E6E7	human large vessel, immortal	125	>500
HM/VEC	human microvessel, normal	80	>500
MS1	human microvessel, immortal	125	>500
BO63	baboon smooth muscle, normal	125	>500
C2C12	mouse skeletal muscle, immortal	75	>1000
L6	rat skeletal muscle, immortal	75	>1000
B16	mouse melanoma, tumor	80	>1000
GMO/E6E7	human skin/fb, immortal	500	1000
SK-MEL31	human melanoma	1000	500
Capan-1	human pancreas, tumor	125	>500
Mia PaCa	human pancreas, tumor	62.5	>500
PC-3	human prostate, tumor	250	>4000
SW1417	human colon, tumor	>1000	ND
LS123	human colon, tumor	>1000	ND

Note: The species, tissue, and whether the cell line has a tumor, normal or transformed phenotype are indicated. The IC_{50} for proliferation and the LSCC are indicated. IC_{50} is defined as the concentration at which proliferation is half-maximal to vehicle only controls. The LSCC is defined as that concentration which results in a significant increase in fluorescence compared to vehicle only-treated controls.

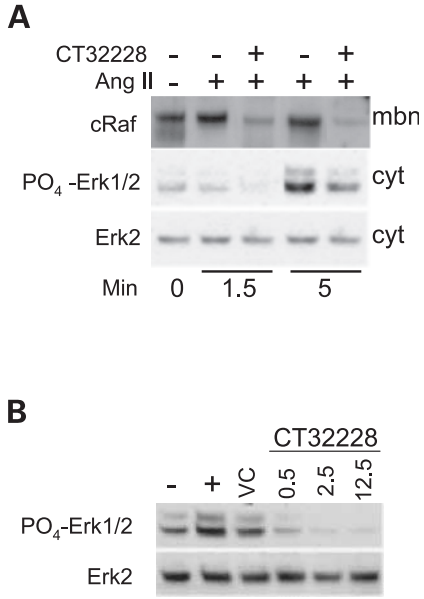

Figure 3. Inhibition of Raf translocation and Erk phosphorylation. **A,** membrane (*mbn*) or cytosolic (*cyt*) fractions of serum-starved HMVEC were either left untreated or pretreated with 500 nM CT32228 for 1 h then stimulated with 10 nM Ang II for 0, 1.5, and 5 min and were analyzed by Western blot. Fractions were normalized for protein content. Lysates were probed for Raf, phosphorylated Erk1/2 and Erk2. **B,** HMVEC were either left untreated or pretreated with CT32228 for 1 h at indicated concentrations then stimulated with 10 nM Ang II for 15 min. Vehicle control (*VC*) is 0.0025% v/v DMSO, equivalent to the concentration in the 12.5 μM CT32228 sample. Whole cell lysates were probed for phosphorylated Erk1/2 and Erk2 as a loading control.

CT32228 Induces Arrest in G_2-M and Subsequent Apoptosis

Because of the antiproliferative and cytotoxic effects of CT32228, we investigated the effects of LPAAT-β inhibition on the cell cycle. IM-9 lymphoblastoid cells were treated with CT32228 at indicated times and concentrations. Flow cytometry was performed on cells stained with Annexin V and on nuclei stained with propidium iodide. By 24 h, more than 50% of the cells were in G_2-M in CT32228-treated cells (Fig. 6A). By 48 h, this proportion had dropped to less than 14%, while the number of hypodiploid cells accounted for nearly 30% of the remaining cells, indicating that it was the cells in G_2-M that became hypodiploid. By 72 h, the G_2-M population was nearly gone. The appearance of hypodiploid cells in the CT32228-treated IM-9 cells was accompanied by a 24% increase in Annexin V-positive cells at 24 h (Fig. 6B). This percentage increased to greater than 85% by 48 h, indicating massive death by apoptosis. Arrest in G_2-M and the appearance of hypodiploid cells were seen with A-20 (B-cell lymphoma), Daudi (Burkitt's lymphoma), Jurkat (T-cell leukemia), HL-60 (acute promyelocytic leukemia), MCF-7 (breast cancer), and DU-145 (prostate cancer) cell lines (Fig. 6C), and in all cases the appearance of hypodiploid cells was accompanied by a large increase in Annexin V-positive cells, indicating that death was apoptotic (data not shown). In contrast, treatment of the primary cells HMVEC or HAVSMC also resulted in arrest of some cells at G_2-M but did not result in Annexin V-positive cells (data not shown) and no hypodiploid cells were seen (Fig. 5D). It appears that in HAVSMC, CT32228 also induced arrest in G_1 as the S-phase population disappeared over time. Alternatively, these cells may have become quiescent as PI staining cannot differentiate between G_0 and G_1. We observed that CT32228 treatment of A20 and Daudi cells caused the appearance of large multinucleated cells (data not shown) as well as the appearance of hyperploid cells (Fig. 6C), indicating that some of these cells were replicating their genomes in a process of mitotic restitution known as endocycles, an adaptive response to mitotic catastrophe (31).

CT32228-Treated Cells Have Activated Cdc2

The accumulation of cells at G_2-M prompted us to look more closely at the signals important for the transition to mitosis. The MPF controls the transition from the G_2 checkpoint into M phase. It is comprised of the cyclin-dependent kinase Cdc2 (also known as Cdk 1) complexed with Cyclin B. Phosphorylation of Cdc2 at tyrosine 15 and threonine 14 inhibits its activity thus causing G_2 arrest. Once Cdc2 becomes activated, by dephosphorylation of T^{14} and Y^{15} via Cdc25 phosphatases, the cell can progress into M phase. Because treatment with CT32228 resulted in accumulation of cells in G_2-M and the appearance of giant multinucleated

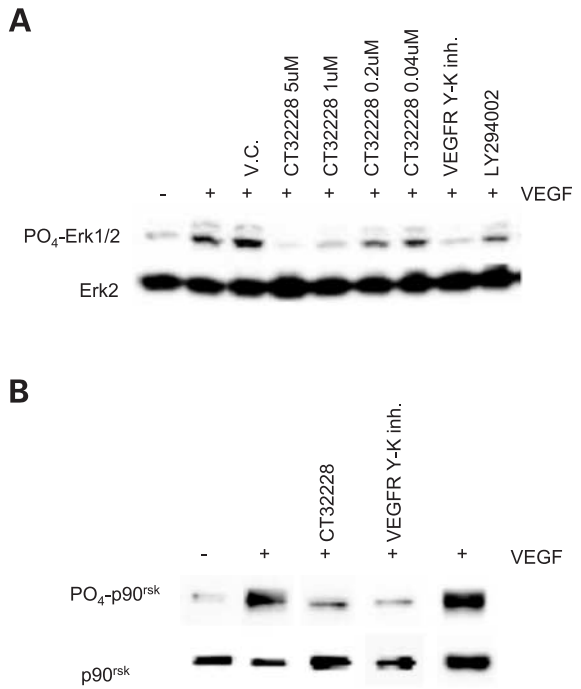

Figure 4. Inhibition of VEGF-stimulated Erk phosphorylation. **A,** serum-starved HMVEC were pretreated with indicated concentrations of CT32228 for 1 h then stimulated for 15 min with 6 ng/ml VEGF plus 1 ng/ml heparin. As a vehicle control (*V.C.*), cells were pretreated with 0.001% v/v DMSO, the concentration equivalent to that in the highest CT32228 sample. As controls, cells were treated with the PI3K inhibitor LY294002 (5 μM) and a VEGF tyrosine kinase inhibitor (25 μM). **B,** samples from **A** were re-probed with antibodies to phosphorylated (T^{359}/S^{363}) and unphosphorylated $p90^{RSK}$. Only the samples with cells pretreated with 0.2 μM CT32228 are shown.

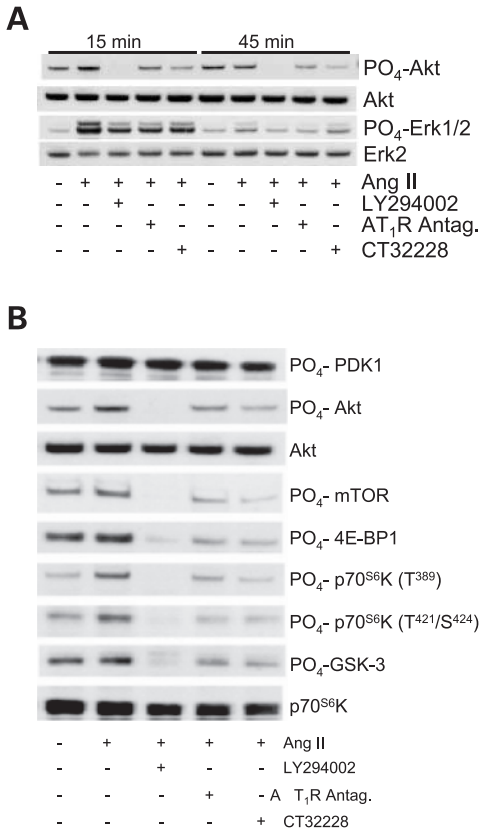

Figure 5. Effects on PI3K/Akt pathway. **A,** serum-starved PAVSMC pretreated for 1 h with 500 nM CT32228 were stimulated with 10 nM Ang II for times indicated. As controls, the cells were either left untreated or were pretreated with 5 μM LY294002 or 100 nM AT_1R antagonist. Whole cell lysates were probed for phosphorylated and unphosphorylated Akt, phosphorylated Erk1/2, and unphosphorylated Erk2. **B,** lysates were probed for phosphorylated forms of PDK1, Akt, m-TOR, 4E-BP1, $p70^{S6K}$, GSK3β, and unphosphorylated Akt and $p70^{S6K}$. Only the 15-min stimulation data are presented here.

cells in some tumor lines, we expected to see that Cdc2 was hyperphosphorylated, indicating arrest at the G_2 checkpoint. Surprisingly, in IM-9 cells, Cdc2 is hypophosphorylated following treatment with CT32228 (Fig. 7A). This suggests that inhibition of LPAAT-β either results in mistimed activation of Cdc2 and improper entry into M phase or the cells arrest after transition from the G_2 checkpoint but before exiting the spindle checkpoint at the end of metaphase when Cdc2 again becomes deactivated. The former seems unlikely as CT32228 treatment had no effect on Cdc25c phosphorylation or Wee1 levels (data not shown). Furthermore, CT32228 treatment does not block T^{161} phosphorylation of Cdc2, a target for Cdc2-activating kinase (CAK), indicating that this step in Cdc2 regulation is not affected (Fig. 7A). Most cell lines tested had hypophosphorylated Cdc2 after treatment with CT32228 (Fig. 7B).

CT32228 Treatment Increases the Mitotic Index in Tumor Cells

Because PI staining is capable of revealing only the genomic content of cells and not the specific stage of cell cycle, we wanted to see if significant numbers of the cells seen to accumulate in G_2-M as judged by PI staining were in fact in M phase. Treatment of tumor cells lines with CT32228 resulted in an increase in the mitotic index (Table 3). In some cells, this increase peaked at 4 h but was sustained for more than 16 h (data not shown). In contrast, although they accumulate in G_2-M following CT32228 treatment, HMVEC did not show significant increases in mitotic bodies, suggesting that these cells remain arrested in G_2.

Treatment with CT32228 Induces Apoptosis

In most cases, improperly timed entry into M phase or prolonged arrest at the spindle checkpoint causes cells to die by apoptotic mechanisms. Therefore, we determined the apoptotic pathways activated in cells treated with CT32228. Treatment of IM-9 cells with 300 nM CT32228 resulted in the expression and activation of Type I receptosome complexes as shown by the activation of Caspase 8 and 10 and the up-regulation of the death receptors DR4 and DR5 (Fig. 8A). Additionally, Type II pathways are activated as Bax expression is increased and Caspase 9 is activated (Fig. 8B). GSK3-β is also activated in these lymphoblastoid cells as previously seen in the Ang II-stimulated PAVSMC. Caspase 3 was activated in all tumor cells tested, but not in HMVEC or HAVSMC (Table 4).

Discussion

Although PA is an important cofactor for a variety of cellular functions, the biochemical origins of PA having discrete functions have not been fully elucidated. LPAAT-α has a uniform tissue distribution and is apparently not up-regulated in tumor cells, suggesting a housekeeping role for this enzyme. LPAAT-β, on the other hand, is differentially expressed in normal tissues and overexpressed in most tumor tissues, which frequently have activated PA-associated signaling pathways. Ectopic overexpression of LPAAT-β in NIH/3T3 cells is associated with proliferation in low serum and tumorigenicity in nude mice. Specific removal of the overexpressed gene reversed these parameters of transformation (23). LPAAT-β is principally located in the ER, although our results suggest that some fraction of LPAAT-β activity is associated with events at the plasma membrane. More work needs to be done to establish if LPAAT-β pools are located in functionally relevant areas apart from the ER.

Because PA is an important cofactor in signaling pathways, we investigated a potential role for LPAAT-β. The MPF is activated in *Xenopus* oocytes by progesterone acting through a cytoplasmic signal transduction pathway involving activation of Erk (26). GVBD was induced when transcripts of constitutively active Raf or Ras were injected into *Xenopus* oocytes, thereby bypassing the upstream signals normally present in the progesterone pathway. Co-injection with LPAAT-β transcripts, but not LPAAT-α, PLD, or the catalytically inactive form of LPAAT-β, augmented induction of GVBD and resulted in greatly enhanced Erk activation. These data suggest that LPAAT-β plays a role in Raf/Ras/Erk signaling.

To further probe the role of LPAAT-β in signaling, we used a member of a class of LPAAT-β isoform-specific inhibitors, CT32228. This compound acts by uncompetitive inhibition of LPA binding (apparent K_i = 47 ± 6 nM) and mixed noncompetitive inhibition of 18:1-CoA binding (because of the nature of this inhibition, the K_i for 18:1-CoA is undetermined). Significantly, CT32228 does not inhibit the ability of PLD1 or PLD2 to hydrolyze phosphatidylcholine (data not shown). Initial biochemical studies have shown that LPAAT-β appears to have a preference for the transfer of oleoyl acyl chains over that of arachidonoyl acyl chains (data not shown), suggesting that LPAAT-β produces molecular species of PA similar to that of PLD (18). Taken together, these findings raise the possibility that at least some of the PA-dependent signaling models may rely on LPAAT-β rather than PLD.

The recruitment of Raf to membranes in some model systems has been shown to require PA (29) and this process is associated with oncogenesis. Activation of Raf involves two distinct steps; translocation as a multisubunit

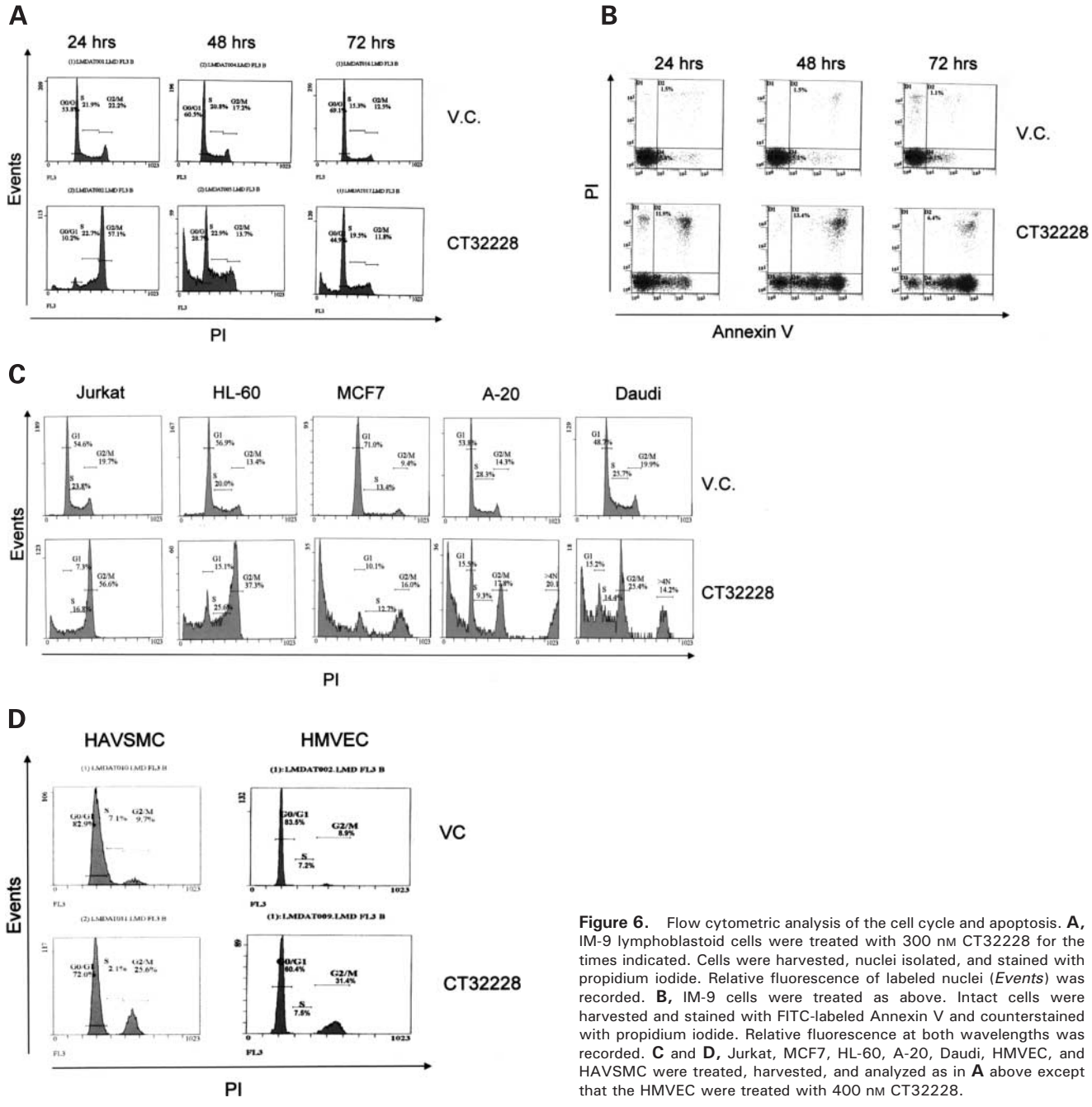

Figure 6. Flow cytometric analysis of the cell cycle and apoptosis. **A,** IM-9 lymphoblastoid cells were treated with 300 nM CT32228 for the times indicated. Cells were harvested, nuclei isolated, and stained with propidium iodide. Relative fluorescence of labeled nuclei (*Events*) was recorded. **B,** IM-9 cells were treated as above. Intact cells were harvested and stained with FITC-labeled Annexin V and counterstained with propidium iodide. Relative fluorescence at both wavelengths was recorded. **C** and **D,** Jurkat, MCF7, HL-60, A-20, Daudi, HMVEC, and HAVSMC were treated, harvested, and analyzed as in **A** above except that the HMVEC were treated with 400 nM CT32228.

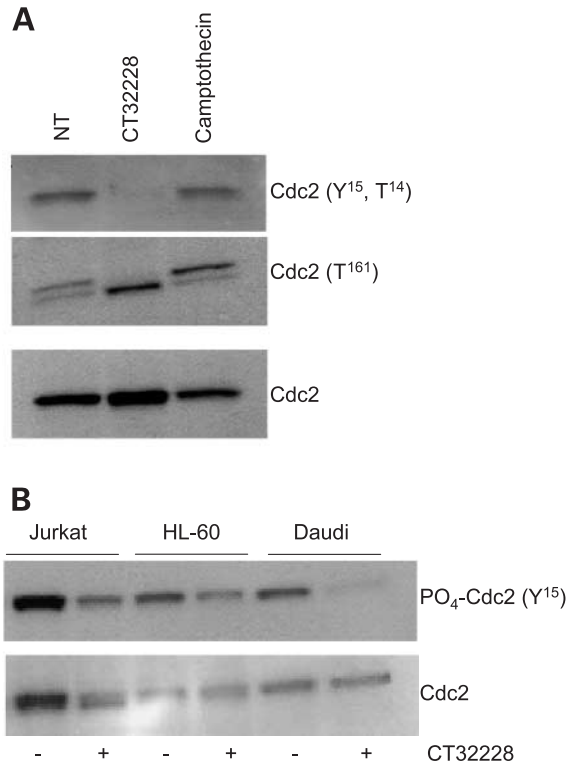

Figure 7. Activation of Cdc2. **A,** IM-9 cells were treated with 300 nM CT32228 for 18 h. As controls, cells were left untreated or treated with the topoisomerase I inhibitor, camptothecin at 25 μM. Whole cell lysates were probed for phosphorylated (*Y^{15}*, *T^{14}*, and *T^{161}*) or unphosphorylated forms of Cdc2. The doublets seen in the Cdc2(T^{161}) image represent phosphorylation of Cdc2 at Y^{15} and T^{14}. **B,** whole cell lysates from Jurkat, HL-60, and Daudi cells either left untreated or treated with 300 nM CT32228 were probed for phosphorylated (Y^{15}, T^{14}) and unphosphorylated Cdc2.

complex to the membrane (32) followed by its activation by Src and Src-like kinases, Ras, and perhaps others (33). PLD has been reported to be an important source of PA for Raf recruitment (34). We used CT32228 to investigate the contribution from LPAAT-β to the PA requirement for Raf recruitment. CT32228 effectively blocks Raf translocation to membranes following stimulation with Ang II. Consistent with this, Erk phosphorylation was inhibited in these cells. Phosphorylation of Raf at S^{261} was not affected by CT32228 (data not shown). Dephosphorylation of this site abrogates 14-3-3 binding, a necessary step for activation of the kinase domain of Raf (35), supporting the idea that LPAAT-β exerts an inhibitory effect on Raf signaling by interfering with translocation rather than on Raf kinase activation events.

Ang II stimulation of VSMC activates the PI3K/Akt pathway by transactivation of the EGFR (30) while Erk is activated in a Ras-dependent manner via EGFR transactivation and by a Ras-independent pathway using PKC (30, 36, 37). This model allowed us to test if events other than Raf recruitment are also affected by inhibition of LPAAT-β. Pretreatment of PAVSMC with CT32228 significantly attenuated phosphorylation of Akt and the downstream effectors $p70^{S6K}$, mTOR, 4E-BP, and GSK3β. It is not clear what role PA plays in the activation of Akt. CT32228 does not inhibit either PDK1 activation or PI3K activity (data not shown). However, a possible connection is suggested by recent work showing that PKCζ, a PKC isoform that requires PA for its activation (10) forms a complex with PDK to activate Akt (38). mTOR is activated by Akt and thus the hypophosphorylation of mTOR in CT32228-treated cells may be due to reduced activity of Akt. However, mTOR also has been reported to require PA for its activation (6). It is unclear if the inhibition of mTOR phosphorylation observed

Table 3. Mitotic index

	VC	CT32228
DU145	15/10	45/10
Daudi	3/10	15/10
A20	1/10	6/10
HMVEC	1/10	1/10
VSMC	0/10	0/10

Note: Cells were treated with 500 nM CT32228 for 16 h. Mitotic index was determined by counting the number of mitotic bodies present in representative HPFs.

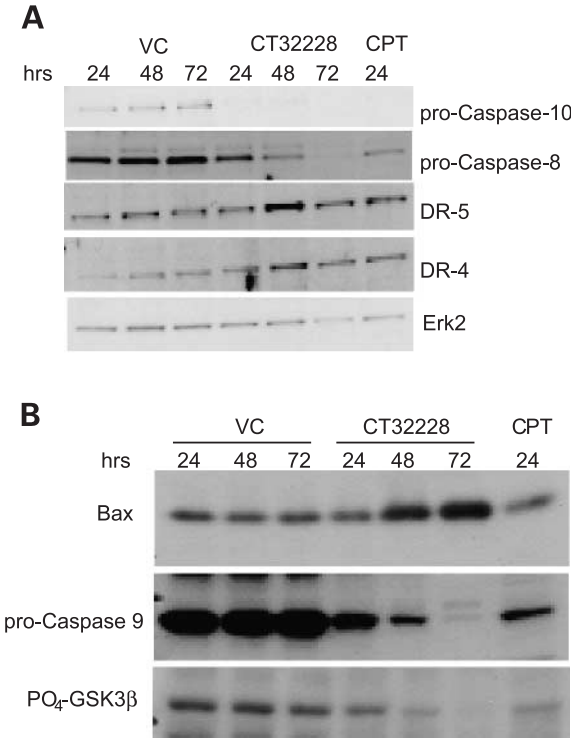

Figure 8. Apoptosis pathways. **A,** IM-9 cells were treated with 300 nM CT32228 for times indicated. As controls, cells were either treated with vehicle only (*VC*; 0.001% v/v DMSO) for the duration of the experiment or were treated with 25 μM camptothecin for 24 h. Whole cell lysates were prepared and probed for pro-Caspase 8 and 10, DR4, and DR5. In this experiment, Erk 2 was used as loading control as the cells were unstimulated and its levels did not change over the duration of the experiment. **B,** IM-9 cells were treated as above and lysates probed for Bax, pro-Caspase 9, and GSK3β.

Table 4. Caspase 3 activation

	16 h	72 h
A-20	40%	60%
Daudi	20%	40%
HMVEC	<5%	30%
PAVSMC	<1%	<1%

Note: DU145, A-20, DAUDI, HMVEC, and BAVSMC were treated with 500 nM CT32228 for the times indicated. Activated Caspase 3 levels were judged by relative nuclear staining by ICC and were scored from 1 to 3. Active Caspase 3 in this table indicates the percentage of nuclei scoring 2–3+.

here is due to this requirement or if it is due to reduced Akt activity or possibly both. When the Burkitt's lymphoma Daudi cell line is treated with CT32228, constitutive mTOR phosphorylation is signficantly inhibited but Akt phosphorylation is only slightly blocked (data not shown), suggesting that LPAAT-β may be the source of the PA required for mTOR activation.

Hypophosphorylation of Cdc2 seen in CT32228-treated cells suggests that inhibition of LPAAT-β results in activated MPF. Because micro-injected LPAAT-β transcripts enhanced constitutively active Raf and Ras-induced GVBD, it is difficult to reconcile the findings that Cdc2 is activated both by ectopic overexpression of LPAAT-β and by the inhibition of its enzymatic activity. However, the exact role of the Ras/Raf/Erk pathway in GVBD is complex and the timing of events is critical. It has been demonstrated that while Ras/Raf/Erk is important for release of G_2 arrest and induction of GVBD in frog oocytes, the same activation in frog eggs results in G_2 arrest (39). Normal vascular endothelial and smooth muscle cells do appear to arrest before entry into M phase. However, in tumor cells, the more likely explanation for our observations of Cdc2 activation is that arrest occurs at the spindle checkpoint, and thus Cdc2 remains in an active state. Our findings with Cdc25c activation, Wee1 levels, T^{161} phosphorylation of Cdc2, and the increase in mitotic index in CT32228-treated tumor cells suggest that arrest occurs at the spindle checkpoint. It may be that some cells undergo G_2 arrest while others arrest in M phase depending on their respective needs for LPAAT-β-derived PA. We found that most tumor cell lines arrest and die by apoptosis irrespective of their p53 status, suggesting that p53-dependent G_2 checkpoint mechanisms are largely unaffected by LPAAT-β inhibition. Furthermore, otherwise genetically identical cells expressing HPV E6E7 genes to inactivate p53 and Rb (40) are not altered in their sensitivity to either the antiproliferative or cytotoxic effects of the compounds (data not shown). In contrast, HMVEC and HAVSMC arrest in G_2, suggesting a role for LPAAT-β-derived PA in release of G_2 arrest in normal cells. Differences in sensitivity to LPAAT-β inhibitors likely reflect differences in requirements for LPAAT-β-derived PA. In as much as PA contributes to a number of pathways, and the dependence on particular pathways varies from cell line to cell line, these differences in proliferative and cytotoxic responses to LPAAT-β inhibition are perhaps not surprising. To the extent that CT32228-resistant cell lines require PA, it seems likely that PLD activity alone is sufficient to accommodate their PA-dependent signaling needs; thus, inhibition of LPAAT-β has little consequence to these cells.

As with all small molecular weight inhibitors, we cannot rule out the possibility that CT32228 and related LPAAT-β-specific inhibitors have additional targets which may account for some of the findings reported here. However, we have used RNAi knockdown of LPAAT-β to recapitulate LPAAT-β inhibitor effects on proliferation, apoptosis, and Ras/Raf/Erk signaling in several tumor cell lines,[1] suggesting that additional targets, if they exist, likely do not mitigate our findings with CT32228.

A variety of phospholipid-derived molecules play significant roles in signaling pathways, including platelet-activating factor, DAG, eicosanoids, phosphoinositides, LPA, and PA. LPAATs have been implicated in some signaling pathways for more than a decade (41); however, only recently have tools become available to elucidate LPAAT-β's specific role. Although our observations suggest interactions of LPAAT-β with the cell signaling apparatus, the full accounting of relevant molecules affected by this enzyme and precise means of their interaction has yet to be elucidated. Because of the demands of poorly regulated growth, tumor cells may come to rely on the function of normal genes in ways that normal cells do not. LPAAT-β is an attractive and novel target in cancer therapeutics that may be among this category of genes.

Acknowledgments

The authors thank David Leung and Ruthanne Naranjo for critical review of the manuscript and Renee McCormick, Jeni Moses, Chris Wallick, Lisa Romero, and Drew Dover for excellent technical assistance.

References

1. West, J., Tompkins, C., Balantac, N., Martin, K., Nudelman, E., Meengs, B., White, T., Bursten, S. L., Coleman, J., Kumar, A., Klein, P., Singer, J. W., and Leung, D. W. Cloning and expression of two human lysophosphatidic acid acyltransferase cDNAs that stimulate cytokine induced signaling responses in cells. DNA Cell Biol., *16:* 691–701, 1997.

2. Schmidt, A., Wolde, M., Thiele, C., Fest, W., Kratzin, H., Podtelejnikov, A. V., Witke, W., Huttner, W. B., and Soling, H. D. Endophilin I mediates synaptic vesicle formation by transfer of arachidonate to lysophosphatidic acid. Nature, *401:* 133–141, 1999.

3. Weigert, R., Silletta, M. G., Spano, S., Turacchio, G., Cericola, C., Colanzi, A., Senatore, S., Mancini, R., Polishchuk, E. V., Salmona, M., Facchiano, F., Burger, K. N., Mironov, A., Luini, A., and Corda, D. CtBP/BARS induces fission of Golgi membranes by acylating lysophosphatidic acid. Nature, *402:* 429–433, 1999.

4. Athenstaedt, K. and Daum, G. Phosphatidic acid, a key intermediate in lipid metabolism. Eur. J. Biochem., *266:* 1–16, 1999.

5. Ghosh, S., Strum, J. C., Sciorra, V. A., Daniel, L., and Bell, R. M. Raf-1

[1] M. Coon, A. Ball, J. Pound, D. Hollenback, and J. W. Singer. RNA: Knockdown of lysophosphatidic acid acyltransferase-beta (LPAAT-β) inhibits proliferation and induces apoptosis in tumor cell lines, submitted for publication.

kinase possesses distinct binding domains for phosphatidylserine and phosphatidic acid. Phosphatidic acid regulates the translocation of Raf-1 in 12-*O*-tetradecanoylphorbol-13-acetate-stimulated Madin-Darby canine kidney cells. J. Biol. Chem., *271:* 8472 – 8480, 1996.

6. Fang, Y., Vilella-Bach, M., Bachmann, R., Flanigan, A., and Chen, J. Phosphatidic acid-mediated mitogenic activation of mTOR signaling. Science, *294:* 1942 – 1945, 2001.

7. Shen, Y., Xu, L., and Foster, D. A. Role for phospholipase D in receptor-mediated endocytosis. Mol. Cell. Biol., *21:* 595 – 602, 2001.

8. Jones, D., Morgan, C., and Cockcroft, S. Phospholipase D and membrane traffic. Potential roles in regulated exocytosis, membrane delivery and vesicle budding. Biochim. Biophys. Acta, *1439:* 229 – 244, 1999.

9. Sergeant, S., Waite, K. A., Heravi, J., and McPhail, L. C. Phosphatidic acid regulates tyrosine phosphorylating activity in human neutrophils: enhancement of Fgr activity. J. Biol. Chem., *276:* 4737 – 4746, 2001.

10. Limatola, C., Schaap, D., Moolenaar, W. H., and van Blitterswijk, W. J. Phosphatidic acid activation of protein kinase C-ζ overexpressed in COS cells: comparison with other protein kinase C isotypes and other acidic lipids. Biochem. J., *3:* 1001 – 1008, 1994.

11. Pawelczyk, T. and Matecki, A. Phospholipase C-δ3 binds with high specificity to phosphatidylinositol 4,5-bisphosphate and phosphatidic acid in bilayer membranes. Eur. J. Biochem., *262:* 291 – 298, 1999.

12. Bechoua, S. and Daniel, L. W. Phospholipase D is required in the signaling pathway leading to p38 MAPK activation in neutrophil-like HL-60 cells, stimulated by *N*-formyl- methionyl-leucyl-phenylalanine. J. Biol. Chem., *276:* 31752 – 31759, 2001.

13. Lee, S. D., Lee, B. D., Han, J. M., Kim, J. H., Kim, Y., Suh, P. G., and Ryu, S. H. Phospholipase D2 activity suppresses hydrogen peroxide-induced apoptosis in PC12 cells. J. Neurochem., *75:* 1053 – 1059, 2000.

14. Banno, Y., Takuwa, Y., Akao, Y., Okamoto, H., Osawa, Y., Naganawa, T., Nakashima, S., Suh, P. G., and Nozawa, Y. Involvement of phospholipase D in sphingosine 1-phosphate-induced activation of phosphatidylinositol 3-kinase and Akt in Chinese hamster ovary cells overexpressing EDG3. J. Biol. Chem., *276:* 35622 – 35628, 2001.

15. Sanjuan, M. A., Jones, D. R., Izquierdo, M., and Merida, I. Role of diacylglycerol kinase α in the attenuation of receptor signaling. J. Cell Biol., *153:* 207 – 220, 2001.

16. Topham, M. K. and Prescott, S. M. Diacylglycerol kinase ζ regulates Ras activation by a novel mechanism. J. Cell Biol., *152:* 1135 – 1143, 2001.

17. Jones, D. R., Sanjuan, M. A., Stone, J. C., and Merida, I. Expression of a catalytically inactive form of diacylglycerol kinase a induces sustained signaling through RasGRP. FASEB J., *16:* 595 – 597, 2002.

18. Hodgkin, M. N., Pettitt, T. R., Martin, A., Michell, R. H., Pemberton, A. J., and Wakelam, M. J. Diacylglycerols and phosphatidates: which molecular species are intracellular messengers? Trends Biochem. Sci., *23:* 200 – 204, 1998.

19. Brodin, L., Low, P., and Shupliakov, O. Sequential steps in clathrin-mediated synaptic vesicle endocytosis. Curr. Opin. Neurobiol., *10:* 312 – 320, 2000.

20. Leung, D. W. The structure and functions of human lysophosphatidic acid acyltransferases. Front. Biosci., *6:* D944 – D953, 2001.

21. Kume, K. and Shimizu, T. cDNA cloning and expression of murine 1-acyl-*sn*-glycerol-3-phosphate acyltransferase. Biochem. Biophys. Res. Commun., *237:* 663 – 666, 1997.

22. Eberhardt, C., Gray, P. W., and Tjoelker, L. W. Human lysophosphatidic acid acyltransferase. cDNA cloning, expression, and localization to chromosome 9q34.3. J. Biol. Chem., *272:* 20299 – 20305, 1997.

23. Bonham, L., Leung, D., White, T., Hollenback, D., Klein, P., Tulinsky, J., Coon, M., de Vries, P., and Singer, J. W. Lysophosphatidic acid acyl transferase-β: a novel target for induction of tumour cell apoptosis through inhibition of kinase signalling pathways. Exp. Opin. Ther. Targets, in press, 2003.

24. Aguado, B. and Campbell, R. D. Characterization of a human lysophosphatidic acid acyltransferase that is encoded by a gene located in the class III region of the human major histocompatibility complex. J. Biol. Chem., *273:* 4096 – 4105, 1998.

25. Chakraborty, T. R., Vancura, A., Balija, V. S., and Haldar, D. Phosphatidic acid synthesis in mitochondria. Topography of formation and transmembrane migration. J. Biol. Chem., *274:* 29786 – 29790, 1999.

26. Fabian, J. R., Morrison, D. K., and Daar, I. O. Requirement for Raf and MAP kinase function during the meiotic maturation of *Xenopus* oocytes. J. Cell Biol., *122A:* 645 – 652, 1993.

27. White, T., Bursten, S. L., Federighi, D., Lewis, R. A., and Nudelman, E. High-resolution separation and quantification of neutral lipid and phospholipid species in mammalian cells and sera by multi-one-dimensional thin-layer chromatography. Anal. Biochem., *258:* 109 – 117, 1998.

28. Gotoh, Y., Masuyama, N., Dell, K., Shirakabe, K., and Nishida, E. Initiation of *Xenopus* oocyte maturation by activation of the mitogen-activated protein kinase cascade. J. Biol. Chem., *270:* 25898 – 25904, 1995.

29. Rizzo, M. A., Shome, K., Watkins, S. C., and Romero, G. The recruitment of Raf-1 to membranes is mediated by direct interaction with phosphatidic acid and is independent of association with Ras. J. Biol. Chem., *275:* 23911 – 23918, 2000.

30. Eguchi, S., Iwasaki, H., Ueno, H., Frank, G. D., Motley, E. D., Eguchi, K., Marumo, F., Hirata, Y., and Inagami, T. Intracellular signaling of angiotensin II-induced p70 S6 kinase phosphorylation at Ser(411) in vascular smooth muscle cells. Possible requirement of epidermal growth factor receptor, Ras, extracellular signal-regulated kinase, and Akt. J. Biol. Chem., *274:* 36843 – 36851, 1999.

31. Erenpreisa, J. and Cragg, M. S. Mitotic death: a mechanism of survival? A review. Cancer Cell Int., *1:*1, 2001.

32. Wartmann, M. and Davis, R. J. The native structure of the activated Raf protein kinase is a membrane-bound multi-subunit complex. J. Biol. Chem., *269:* 6695 – 6701, 1994.

33. Morrison, D. K. and Cutler, R. E. The complexity of Raf-1 regulation. Curr. Opin. Cell Biol., *9:* 174 – 179, 1997.

34. Rizzo, M. A., Shome, K., Vasudevan, C., Stolz, D. B., Sung, T. C., Frohman, M. A., Watkins, S. C., and Romero, G. Phospholipase D and its product, phosphatidic acid, mediate agonist-dependent raf-1 translocation to the plasma membrane and the activation of the mitogen-activated protein kinase pathway. J. Biol. Chem., *274:* 1131 – 1139, 1999.

35. Yip-Schneider, M. T., Miao, W., Lin, A., Barnard, D. S., Tzivion, G., and Marshall, M. S. Regulation of the Raf-1 kinase domain by phosphorylation and 14-3-3 association. Biochem. J., *351:* 151 – 159, 2000.

36. Eguchi, S., Numaguchi, K., Iwasaki, H., Matsumoto, T., Yamakawa, T., Utsunomiya, H., Motley, E. D., Kawakatsu, H., Owada, K. M., Hirata, Y., Marumo, F., and Inagami, T. Calcium-dependent epidermal growth factor receptor transactivation mediates the angiotensin II-induced mitogen-activated protein kinase activation in vascular smooth muscle cells. J. Biol. Chem., *273:* 8890 – 8896, 1998.

37. Takahashi, T., Kawahara, Y., Okuda, M., Ueno, H., Takeshita, A., and Yokoyama, M. Angiotensin II stimulates mitogen-activated protein kinases and protein synthesis by a Ras-independent pathway in vascular smooth muscle cells. J. Biol. Chem., *272:* 16018 – 16022, 1997.

38. Hodgkinson, C. P., Sale, E. M., and Sale, G. J. Characterization of PDK2 activity against protein kinase B γ. Biochemistry, *41:* 10351 – 10359, 2002.

39. Walter, S. A., Guadagno, S. N., and Ferrell, J. E., Jr. Activation of Wee1 by p42 MAPK *in vitro* and in cycling *Xenopus* egg extracts. Mol. Biol. Cell, *11:* 887 – 896, 2000.

40. Halbert, C. L., Demers, G. W., and Galloway, D. A. The E7 gene of human papillomavirus type 16 is sufficient for immortalization of human epithelial cells. J. Virol., *65:* 473 – 478, 1991.

41. Bursten, S. L., Harris, W. E., Bomsztyk, K., and Lovett, D. Interleukin-1 rapidly stimulates lysophosphatidate acyltransferase and phosphatidate phosphohydrolase activities in human mesangial cells. J. Biol. Chem., *266:* 20732 – 20743, 1991.